Discover Oncology

ANALYSIS Open Access

Decoding epithelial-T cell interactions in colorectal cancer through single-cell and spatial transcriptomics

Rentao Yu[1†], Xinyu Lu[2†] and Zhuangzhuang Yue[3*]

[†]Rentao Yu and Xinyu Lu contributed equally.

*Correspondence:
Zhuangzhuang Yue
871588375@qq.com
[1]Department of Gastrointestinal Surgery, Chongming Hospital Affiliated to Shanghai University of Medicine and Health Sciences, Shanghai 202150, China
[2]Infusion Room, Chongming Hospital Affiliated to Shanghai University of Medicine and Health Sciences, Shanghai 202150, China
[3]Department of Oncology, Chongming Hospital Affiliated to Shanghai University of Medicine and Health Sciences, No. 25, Nanmen Road, Chengqiao Town, Chongming District, Shanghai 202150, China

Abstract

Background Colorectal cancer (CRC) is a heterogeneous malignancy shaped by genetic alterations and immune microenvironmental interactions. While single-cell RNA sequencing (scRNA-seq) has uncovered diverse epithelial and T cell subsets, the spatial architecture of their crosstalk remains poorly understood.

Methods We integrated scRNA-seq and spatial transcriptomics data from 36 CRC patients to comprehensively characterize epithelial and T cell heterogeneity, differentiation dynamics, and intercellular communication networks. Data preprocessing and integration were conducted using Seurat and Harmony. Cell trajectory inference was performed via CytoTRACE and Slingshot. Ligand-receptor signaling was assessed using CellChat, while spatial mapping was achieved using CellTrek.

Results Nine epithelial and eight T cell subpopulations were identified, each exhibiting distinct transcriptional states, CNV burdens, and pseudotime trajectories. $CD8^+$ T_GZMK cells displayed tumor-specific activation signatures and engaged in enriched communication with epithelial subsets through CEACAM, APP, and MIF signaling pathways. Spatial transcriptomics confirmed the in situ colocalization of $CD8^+$ T_GZMK cells with $PTP4A3^+$ epithelial cells in tumor regions, revealing spatially organized epithelial–immune niches. These interactions suggest potential mechanisms of immune modulation and tumor progression.

Conclusion This study provides an integrative single-cell and spatial atlas of CRC, revealing structured epithelial–T cell communication and spatial architecture within the tumor microenvironment. Our findings offer novel insights into immune-epithelial crosstalk and identify signaling pathways that may serve as therapeutic targets or biomarkers for CRC precision treatment.

Keywords Colorectal cancer, Single-cell RNA sequencing, Spatial transcriptomics, Epithelial cell, T cell, Tumor microenvironment

1 Introduction

Colorectal cancer (CRC) is one of the most prevalent malignancies worldwide and remains a leading cause of cancer-related mortality [1]. Despite advances in screening and treatment, the overall survival of advanced CRC patients remains unsatisfactory [2]. Traditionally, CRC development has been attributed to stepwise genetic and epigenetic alterations, including mutations in APC, KRAS, TP53, and microsatellite instability [3]. These classical pathways drive the adenoma-carcinoma sequence and reshape the tumor microenvironment (TME), enabling immune evasion and tumor progression [4].

Recent advances in single-cell RNA sequencing (scRNA-seq) have provided unprecedented insights into the cellular heterogeneity within CRC [5]. Studies have delineated distinct subsets of epithelial cells, including tumor stem-like cells and inflammatory epithelial populations, revealing transcriptional programs that support tumor growth and plasticity [6]. In parallel, single-cell profiling of tumor-infiltrating lymphocytes has highlighted the functional diversity and exhaustion states of T cell populations in CRC, suggesting complex roles of adaptive immunity in both anti-tumor responses and immune tolerance [7, 8].

However, a comprehensive understanding of the interaction between epithelial cells and T cells in the CRC microenvironment remains lacking. In particular, the spatial context in which these interactions occur is poorly characterized. Given the limitations of scRNA-seq in capturing spatial information, spatial transcriptomics has emerged as a powerful tool to bridge this gap by preserving tissue architecture while enabling transcriptome-wide profiling [9]. In this study, we integrated single-cell and spatial transcriptomic analyses to systematically investigate epithelial-T cell crosstalk in CRC. Our findings aim to elucidate key ligand-receptor interactions and microenvironmental niches that may drive immune modulation and tumor evolution, ultimately identifying potential biomarkers and therapeutic targets for improved CRC diagnosis and treatment.

2 Materials and methods

2.1 Data acquisition

Single-cell RNA sequencing (scRNA-seq) datasets were sourced from the Gene Expression Omnibus (GEO) under accession number GSE132465 [10] and GSE144735 [10] (https://www.ncbi.nlm.nih.gov/geo/). In addition, a portion of the samples were obtained from the EMBL-ENI database under access number E-MTAB-8107 (https://www.omicsdi.org/dataset/biostudies-arrayexpress/E-MTAB-8107). All scRNA-seq data were composed of 36 CRC patients.

2.2 Single-cell data processing and analysis

All scRNA-seq data were processed using the Seurat R package (version 4.3.0.1) [11]. Standard preprocessing steps were applied, including quality control, normalization, dimensionality reduction, clustering, and data visualization. To address batch effects across different samples and tissue types, we employed the Harmony algorithm (v0.1.1) [12]. Principal component analysis (PCA) was conducted for feature reduction, followed by visualization via uniform manifold approximation and projection (UMAP).

2.3 Trajectory inference

Cellular differentiation states were inferred using the CytoTRACE2 package (v1.0.0) to assess cell potency [13]. The Potency Score, computed by the CytoTRACE R package, serves as a metric to evaluate the "stemness" or developmental immaturity of cells. Its calculation principle is based on the observation that more differentiated and specialized cells exhibit a more complex gene expression profile, whereas more naive and potent cells, such as stem cells, display a relatively simpler gene expression profile. A higher score indicates a more primitive, undifferentiated, and plastic cell state, while a lower score reflects a more mature and specialized cellular phenotype. Lineage reconstruction and trajectory inference were performed with the Slingshot package (v2.8.0) [14], enabling the identification of potential developmental paths within the cellular populations.

2.4 Copy number variation analysis

To predict chromosomal copy number variations (CNVs) from from the single-cell transcriptomic data, we utilized the inferCNV algorithm [15]. The CNV scores generated by the InferCNV R package serve as a comprehensive metric, where a higher value indicates greater extent and magnitude of copy number alterations in the genome of a cell or cell population compared to normal diploid cells. This is a hallmark feature of malignant tumor cells. Researchers utilize CNV scores to identify malignant cells exhibiting significant genomic instability from large-scale single-cell datasets. This method allowed us to distinguish malignant epithelial cells from non-malignant populations based on large-scale CNV profiles.

2.5 Functional enrichment analysis

Differentially expressed genes (DEGs) identified from various clusters were subjected to functional enrichment using the clusterProfiler R package [16, 17]. Both Gene Ontology (GO) and KEGG pathway databases were queried to uncover relevant biological processes and signaling cascades.

2.6 Cell-cell communication analysis

We reconstructed intercellular communication networks using the CellChat framework (v2.1.2) [18]. This approach identified significant ligand–receptor interactions across cellular subtypes, shedding light on the crosstalk within the tumor immune microenvironment.

2.7 Metabolic interaction profiling

To characterize metabolic interaction, particularly between epithelial and fibroblast subset, we applied the MEBOCOST algorithm [19]. This model predicts metabolite-mediated signaling based on transcriptional activity, providing insights into metabolic flux within the tumor niche.

2.8 Spatial transcriptomics integration

Spatial distribution of cell types was inferred through CellTrek (v0.0.94) [20], which integrates scRNA-seq profiles with spatial transcriptomic data. This analysis enabled

high-resolution mapping of cellular localization and colocalization patterns in both malignant and adjacent normal tissues.

3 Results

3.1 Single-cell transcriptomic landscape and cellular heterogeneity in colorectal cancer

To elucidate the cellular composition of CRC and adjacent normal tissues, scRNA-seq was conducted across two independent datasets. After quality control and batch correction, cells were projected onto a UMAP plot (Fig. 1A). Unsupervised clustering identified different major cell populations based on canonical marker genes (Fig. 1B). These cell types were annotated and compared between tumor and normal samples, showing

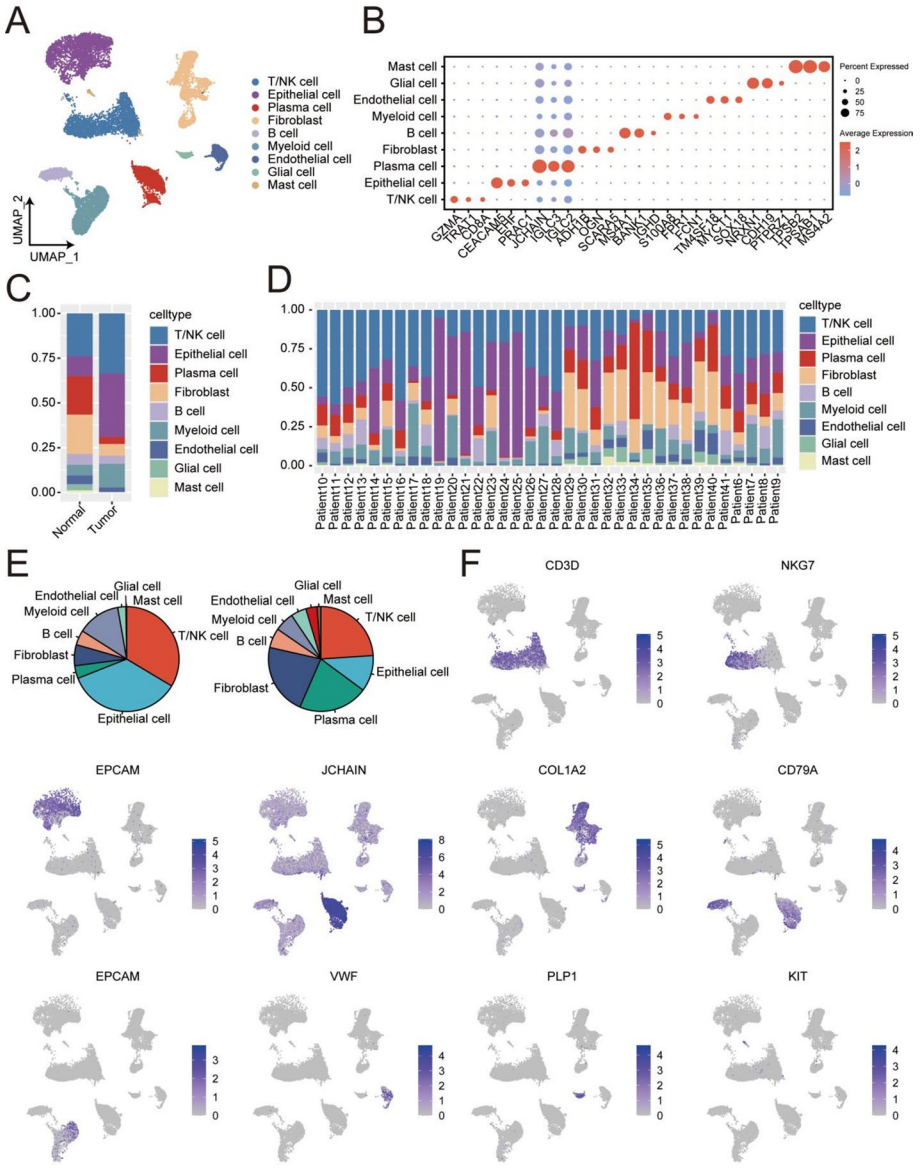

Fig. 1 Single-cell transcriptomic profiling reveals cellular heterogeneity in colorectal cancer and adjacent normal tissues. **A** UMAP plot showing unsupervised clustering of cells from two integrated scRNA-seq datasets. **B** Bubble plot displaying canonical marker genes across the nine major cell types. **C** Proportion of the nine cell types between tumor and normal tissue groups. **D** Bar plot showing the distribution of cell types across individual patients. **E** Pie charts illustrating the proportion of epithelial and non-epithelial cells in tumor and normal tissues. **F** Feature plots showing expression of representative marker genes for each cell type on UMAP

differential distribution of cell populations across conditions (Fig. 1C). Bar plots further illustrated inter-patient heterogeneity in cell subset composition, highlighting patient-specific cell-type enrichment (Fig. 1D). Pie charts depicted the proportion of epithelial and non-epithelial cells in tumor and normal tissues, revealing altered cellular distribution within the tumor microenvironment (Fig. 1E). Feature plots showed the expression patterns of key marker genes across the identified cell populations, supporting their accurate annotation (Fig. 1F).

3.2 Characterization of epithelial cell subpopulations and lineage trajectories

Focusing on epithelial cells, we performed sub-clustering and dimensionality reduction. UMAP visualization showed clear segregation of epithelial subtypes (Fig. 2A). Each subtype displayed distinct proportional abundance and cell counts across tumor and normal tissues (Fig. 2B). Bubble plots of marker gene expression confirmed the molecular identity of these epithelial subclusters (Fig. 2C). CNV analysis using inferred copy number variation scores revealed differential genomic instability among epithelial subtypes (Fig. 2D). The differentiation potential of each epithelial subtype was assessed by Potency Score estimation, with observable differences among clusters. Among them, MKI67 + Epi exhibited the highest differentiation potential, while ZG16 + Epi showed the lowest (Figs. 2E–F). Pseudotime trajectory analysis revealed three distinct lineage branches, suggesting divergent differentiation paths within the epithelial compartment (Fig. 2G). We performed GO and KEGG enrichment analyses on the PTP4A3 + epithelial subpopulation and observed significant enrichment in pathways including negative regulation of apoptotic signaling, epithelial cell proliferation, epithelial cell migration, and NF-kB signaling (Figs. 2H–I). Furthermore, clinical correlation analysis revealed that the abundance of PTP4A3 + epithelial cells was higher in Stage III and IV patients compared to those in Stage I and II, indicating a strong association between this subpopulation and poor patient prognosis (Figs. 2J).

3.3 T cell heterogeneity and functional specialization

T cell subsets were further dissected through scRNA-seq analysis. UMAP projection delineated eight T cell clusters (Fig. 3A), and corresponding bar plots indicated their relative abundance and count in tumor and normal samples (Fig. 3B). Figure 3C displays the top five highly expressed genes in each T cell subset, demonstrating heterogeneity among T cell populations and suggesting distinct functional properties across different subpopulations. Gene ontology (GO) enrichment analysis was conducted for $CD8^+$ T_GZMA and $CD8^+$ T_GZMK subtypes, revealing functional specialization between these two effector populations (Figs. 3D–E). Comparative functional analysis of $CD8^+$ T_GZMK cells in tumor versus normal tissues showed distinct activation and immune response profiles (Fig. 3F). Further, pseudotime inference indicated four developmental trajectories within the T cell compartment, pointing to complex T cell differentiation dynamics (Fig. 3G).

3.4 Cell-cell communication between epithelial and T cell subsets in colorectal cancer environment

To investigate intercellular communication patterns, cell-cell interaction analyses were performed. The number of predicted interactions between epithelial and T cell subsets

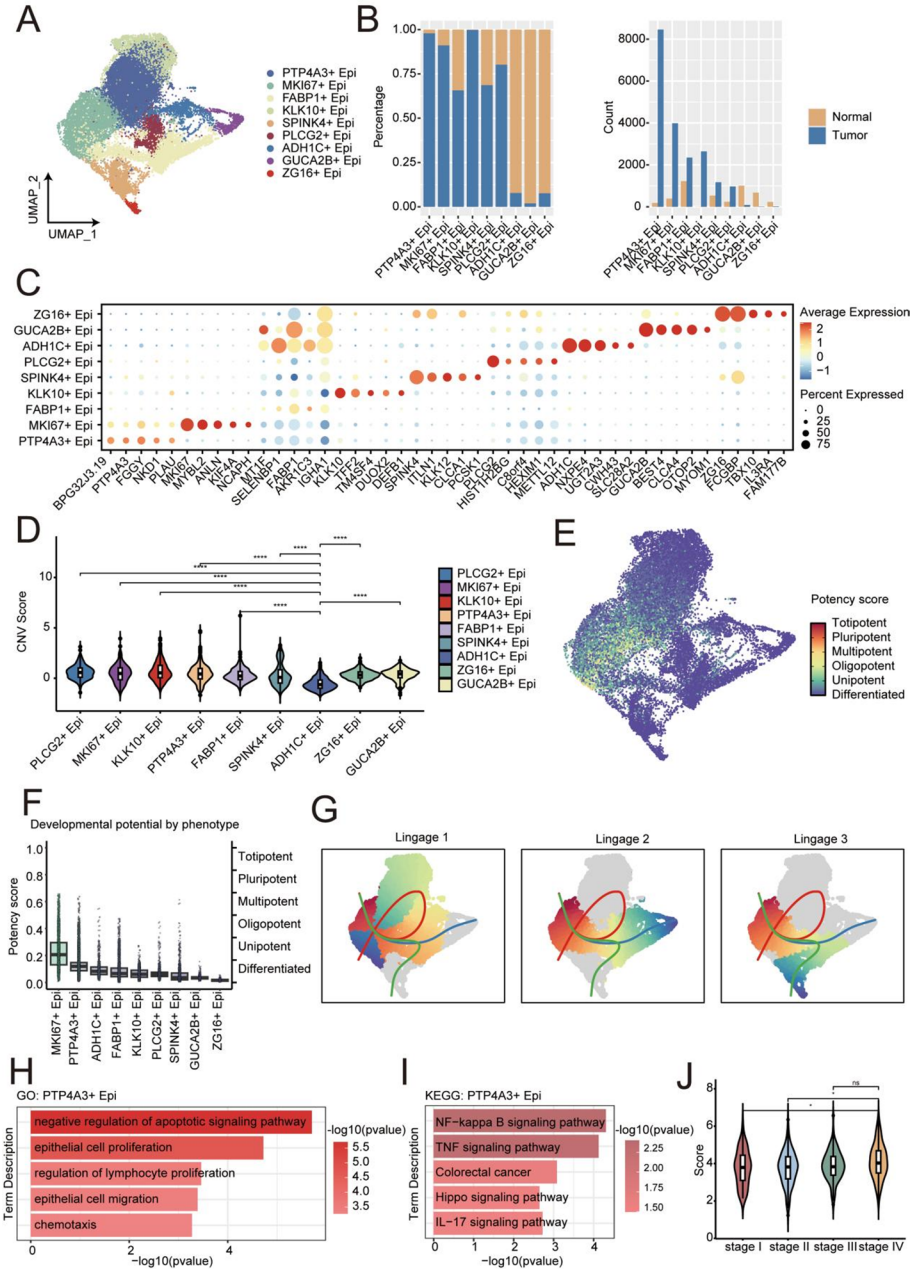

Fig. 2 Identification and characterization of epithelial cell subpopulations in colorectal cancer. **A** UMAP visualization of epithelial cell clustering, identifying nine epithelial subtypes. **B** Bar plot indicating the proportion and number of each epithelial subtype in tumor and normal tissues. **C** Bubble plot showing marker gene expression across epithelial subtypes. **D** Violin plot representing CNV scores across epithelial subtypes. **E** Potency scores for each epithelial subtype inferred by CytoTRACE. **F** Summary of differentiation potential, showing MKI67$^+$ Epi as the most potent and ZG16$^+$ Epi as the most differentiated subtype. **G** Lineage trajectories of epithelial cells inferred by Slingshot, revealing three distinct differentiation branches. **H** GO enrichment analysis of PTP4A3 + Epi. **I** KEGG enrichment analysis of PTP4A3 + Epi. **J** Abundance score of the PTP4A3 + Epi subgroup in CRC patients at different stages

in tumor and normal samples was quantified, showing marked differences in interaction intensity (Fig. 4A). Differential interaction analysis highlighted tumor-specific alterations in communication pathways across multiple cell types (Fig. 4B). Focusing on CD8$^+$ T_GZMK cells, bubble plots demonstrated various epithelial subtypes communication with them (Fig. 4C). Furthermore, the interaction of CD8$^+$T_GZMK cells with different

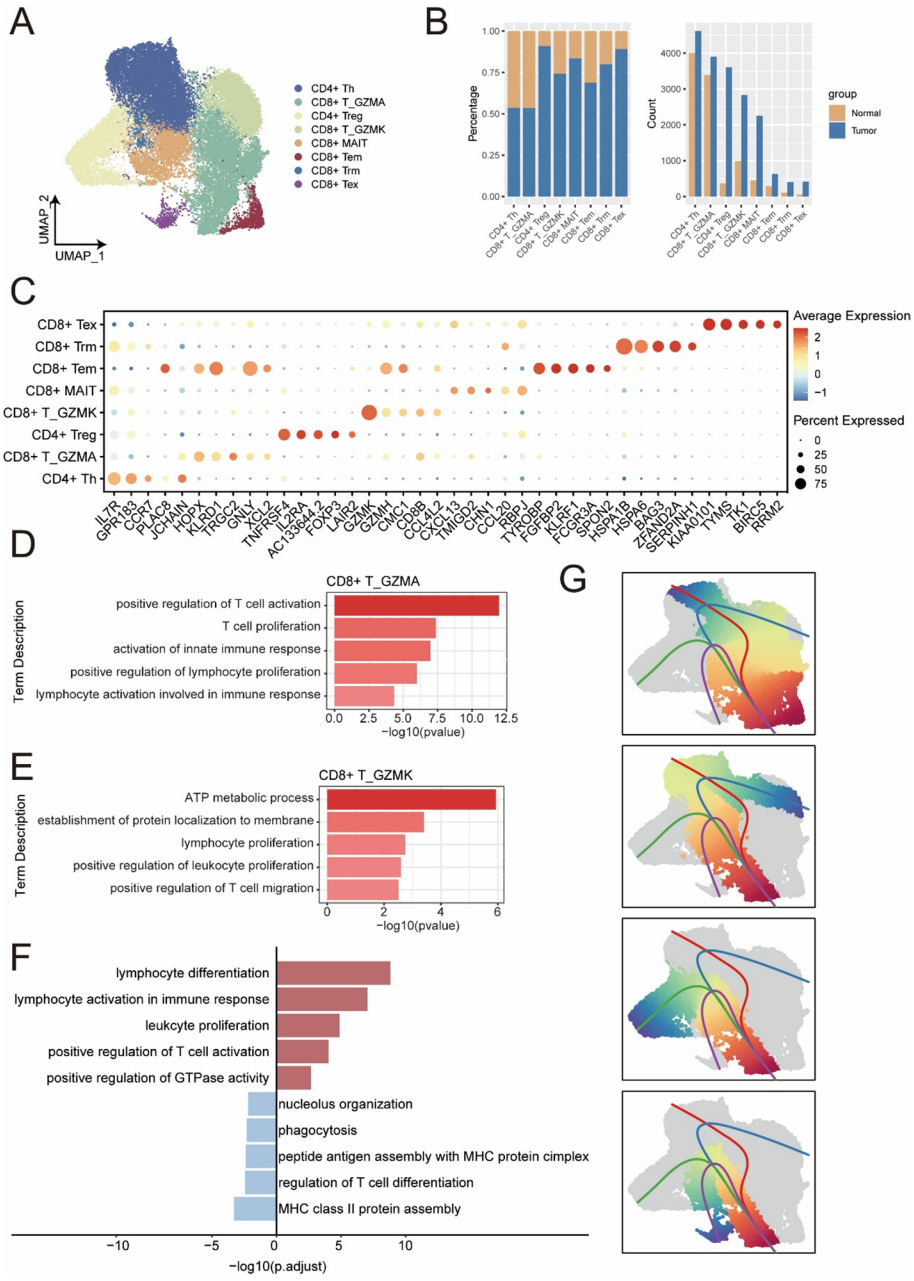

Fig. 3 Dissection of T cell heterogeneity and functional states in colorectal cancer. **A** UMAP plot showing clustering of T cells into eight distinct subsets. **B** Bar plot comparing the abundance and number of each T cell subset in tumor and normal samples. **C** Bubble plot illustrating marker gene expression profiles of T cell subsets. **D** GO enrichment results for CD8⁺ T_GZMA and CD8⁺ T_GZMK subsets. **E** Bar plots showing enriched GO terms for each of the two CD8⁺ subtypes. **F** Comparative functional profiling of CD8⁺ T_GZMK cells between tumor and normal tissues. **G** Pseudotime trajectories of T cells showing four developmental branches

epithelial subtypes was assessed in turn (Fig. 4D). Three signaling pathways—CEACAM, PARs, and CypA—were notably enriched in interactions between CD8⁺ T_GZMK cells and epithelial subtypes, with distinct patterns observed between tumor and normal tissues (Figs. 4E–G). These pathways may mediate key immunomodulatory processes in the tumor microenvironment.

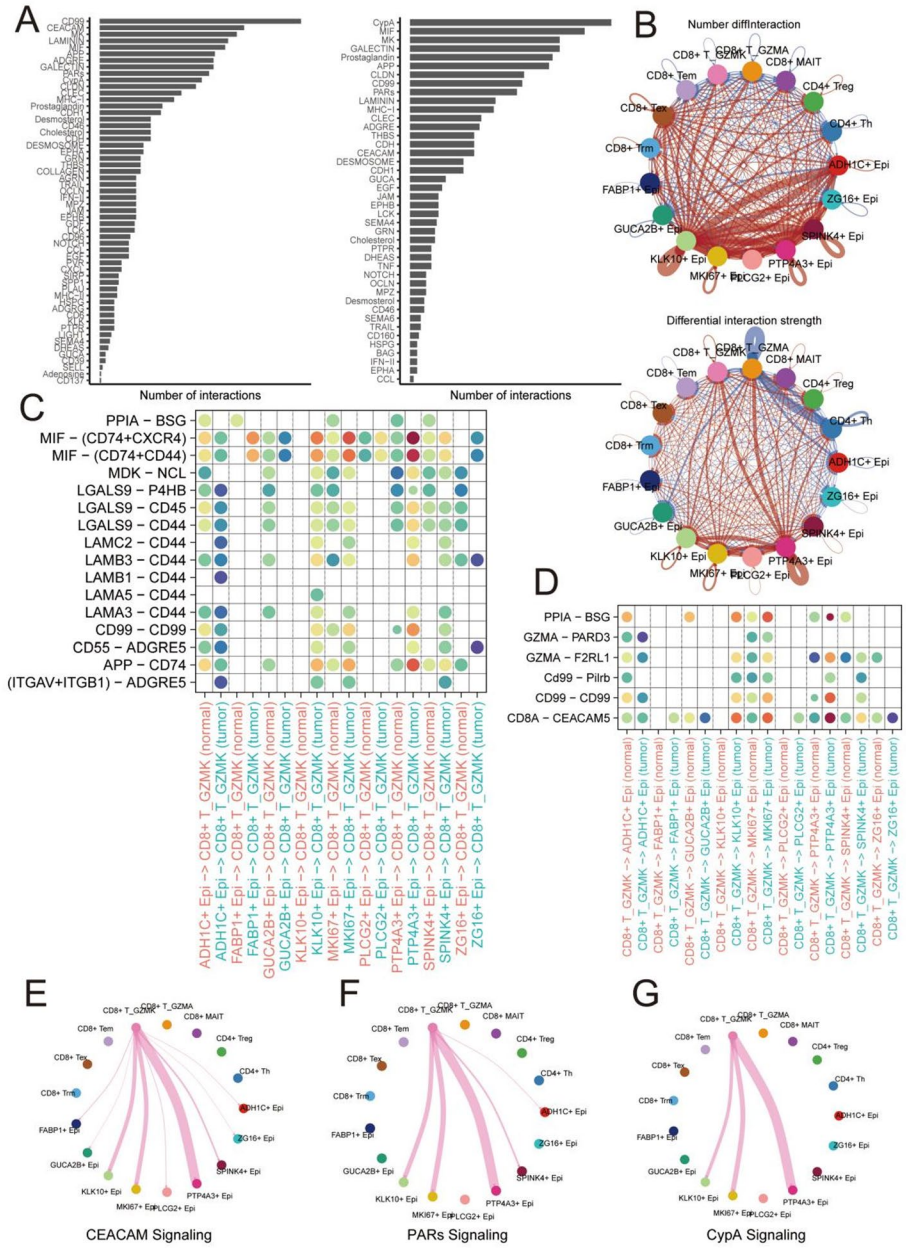

Fig. 4 Tumor-specific epithelial–T cell communication landscape in colorectal cancer. **A** Number of predicted cell-cell interactions between epithelial and T cell subsets in tumor and normal tissues. **B** Differential interaction analysis highlighting altered signaling pathways between tumor and normal conditions. **C** Bubble plot showing ligand–receptor interactions from epithelial subtypes to CD8⁺ T_GZMK cells. **D** Bubble plot showing interactions from CD8⁺ T_GZMK cells to epithelial subtypes. **E** Communication via CEACAM signaling pathway between CD8⁺ T_GZMK and epithelial subsets. **F** PARs pathway-mediated interactions between CD8⁺ T_GZMK and epithelial subtypes. **G** CypA signaling pathway interactions between CD8⁺ T_GZMK and epithelial cells

3.5 Colocalization of epithelial and T cell subsets using spatial transcriptomic analysis

To validate the single-cell findings spatially, spatial transcriptomics was performed on samples from two CRC patients. Spatial clustering of transcriptomic profiles revealed localized expression domains (Fig. 5A and Fig. 5C). In addition, cell type composition and spatial distribution were visualized (Fig. 5B and Fig. 5D). Spatial deconvolution of epithelial and T cell subsets demonstrated their respective localization patterns, confirming their spatial co-occurrence in tumor tissues (Figs. 5E–F). Notably, CD8⁺

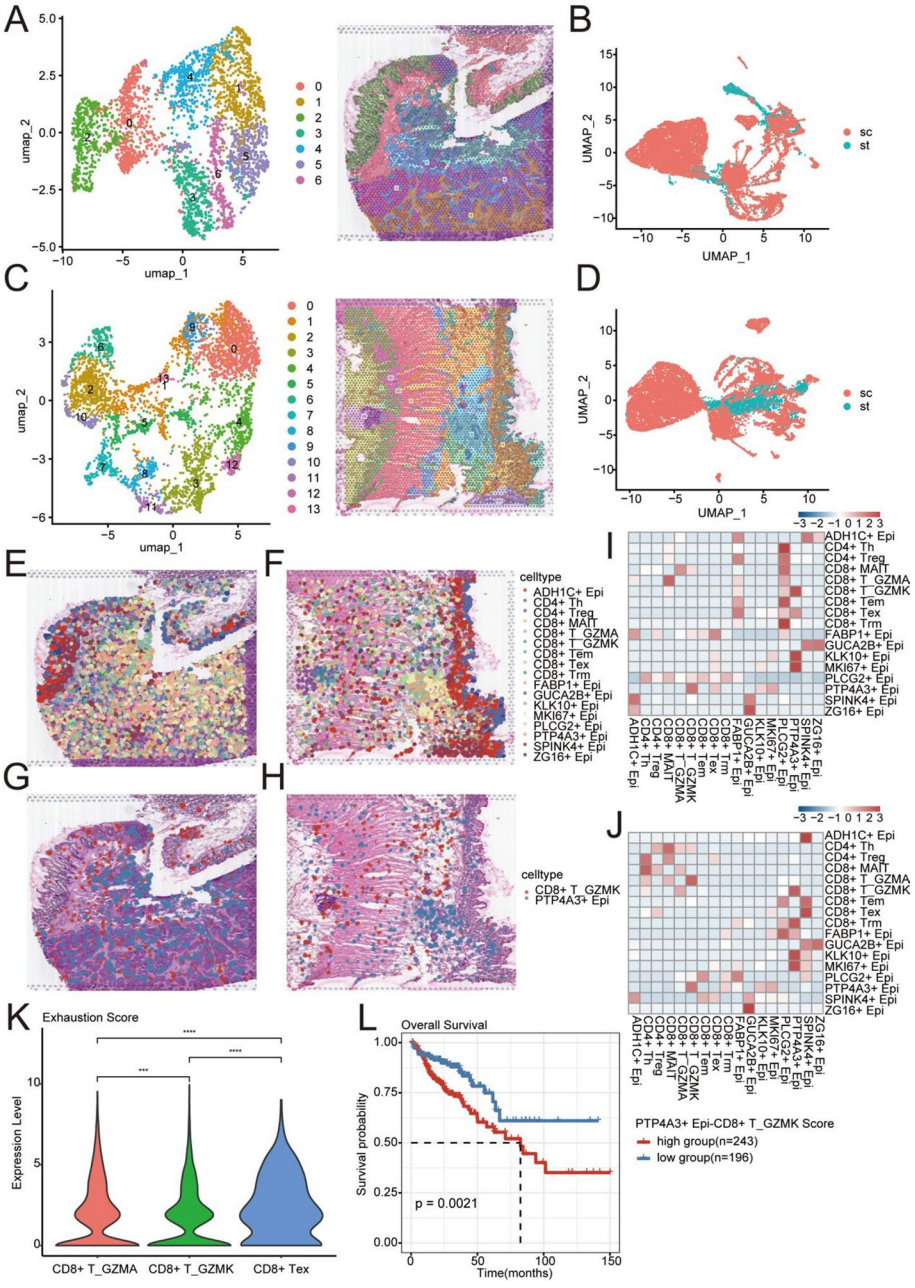

Fig. 5 Spatial transcriptomics confirms colocalization of CD8⁺ T cells and epithelial subsets in colorectal tumors. **A** UMAP projection of spatial transcriptomics from CRC patient 1 showing tissue structure. **B** Data type distribution across spatial transcriptomic sections. **C** UMAP plot of spatial transcriptomic data from CRC patient 2. **D** Data type distribution across tissue sections. **E–F** Spatial deconvolution showing the location of epithelial and T cell subsets in CRC tissue. **G–H** Spatial colocalization of CD8⁺ T_GZMK cells and PTP4A3⁺ epithelial cells within tumor regions. **I–J** Spatial domain analysis of epithelial cell subsets and T cell subsets. **K** Violin plot showing the exhaustion scores of CD8 + T_GZMA, CD8 + T_GZMK, and CD8 + Tex subsets. **L** K–M curve demonstrating the association between PTP4A3 + Epi/CD8 + T_GZMK co-localization and patient prognosis

T_GZMK cells were found to colocalize with the PTP4A3⁺ epithelial subtype within the tumor niche, supporting potential cell-cell interactions in situ (Fig. 5H). Figure 5I–J demonstrate the spatial neighborhood between epithelial cell subsets and T cell subsets, further quantifying the co-localization between CD8 + T_GZMK and PTP4A3 + Epi. To explore functional changes in CD8 + T_GZMK, we evaluated its exhaustion score and

found it to be significantly higher than that of CD8 + T_GZMA but significantly lower than that of CD8 + Tex, suggesting that PTP4A3 + Epi promotes the functional exhaustion of CD8 + T_GZMK (Fig. 5K). In addition, we also explored the association between PTP4A3 + Epi/CD8 + T_GZMK co-localization and patient prognosis and found that patients with a high PTP4A3 + Epi/CD8 + T_GZMK co-localization score had a significantly worse prognosis compared to those with a low score (Fig. 5L).

4 Discussion

In this study, we employed integrated single-cell and spatial transcriptomic analyses to comprehensively characterize the cellular composition and intercellular interactions within CRC tissues and their adjacent normal counterparts. Our results revealed substantial heterogeneity among epithelial and T cell populations, including the identification of distinct subclusters with unique transcriptional and functional profiles. Importantly, we uncovered altered cell-cell communication patterns between epithelial cells and T lymphocytes, particularly involving $CD8^+$ T_GZMK cells, and highlighted spatial colocalization of these interactions within the tumor microenvironment. These findings provide new insights into the immune landscape and cellular organization of CRC, offering potential implications for biomarker discovery and therapeutic targeting.

Our analysis of epithelial cells revealed nine distinct subpopulations, each characterized by specific marker gene expression and divergent genomic and functional properties. Among these, the $MKI67^+$ Epi cluster displayed high differentiation potential, indicative of proliferative and possibly stem-like features, while the $ZG16^+$ Epi subtype exhibited a more differentiated state. CNV profiling further distinguished malignant from non-malignant epithelial cells, supporting previous findings that chromosomal instability is a hallmark of epithelial transformation in CRC [21]. Compared with earlier single-cell studie, which highlighted the existence of tumor stem-like [22] and inflammatory epithelial states [23], our results extend this knowledge by integrating differentiation trajectory and potency scores, thereby revealing developmental hierarchies and transition dynamics among epithelial subsets. Additionally, our spatial transcriptomic integration provides in situ validation of epithelial subtype localization, a dimension often missing in prior work relying solely on dissociated single-cell data [24].

The characterization of T cell populations uncovered eight functionally distinct subsets, including $CD8^+$ T_GZMA and $CD8^+$ T_GZMK clusters. GO enrichment and pseudotime analyses suggested that these T cell subsets are not only phenotypically different but also functionally and developmentally divergent. The $CD8^+$ T_GZMK subset, in particular, exhibited distinct functional states in tumor versus normal tissues, indicating context-dependent immune modulation. These findings are in line with previous work demonstrating the role of cytotoxic T cells [25] and their exhaustion profiles [26] in CRC, but our study further resolves the developmental continuum and potential plasticity of these cells. Furthermore, by integrating spatial transcriptomics, we confirmed the tissue localization of T cell subsets, providing spatial context to their functional states—an advancement over earlier studies limited to transcriptomic or surface marker-based profiling [25].

A central finding of this study is the identification of altered intercellular communication between epithelial and T cell subsets in the CRC microenvironment. Using CellChat analysis, we detected substantial differences in the quantity and quality of

ligand-receptor interactions between tumor and normal tissues. Notably, $CD8^+$ T_GZMK cells showed enriched signaling interactions with multiple epithelial subtypes through pathways such as CEACAM, APP, and MIF, which are known to participate in immune modulation [27], cell adhesion [28], and inflammatory signaling [29]. Prior studies have suggested the immunosuppressive role of CEACAM family proteins in CRC [30], but few have detailed their involvement in epithelial–T cell crosstalk at single-cell resolution. Our work not only confirms these associations but also demonstrates spatial colocalization of $CD8^+$ T_GZMK and $PTP4A3^+$ epithelial cells within tumor niches. This spatial evidence supports a functional link between cellular proximity and communication, a crucial aspect often overlooked in scRNA-seq-based studies. Furthermore, these interactions may underpin mechanisms of immune escape or suppression, warranting further experimental validation.

Despite the comprehensive nature of our study, several limitations should be acknowledged. First, although we analyzed scRNA-seq data from a substantial number of CRC patients, the sample size for spatial transcriptomics was limited to two individuals, potentially restricting generalizability. Second, while our computational analyses suggest active signaling pathways and cellular crosstalk, these interactions are inferred based on gene expression and require functional validation using in vitro or in vivo models. Third, the resolution of current spatial transcriptomics technologies does not allow single-cell precision, which may lead to inaccuracies in colocalization inference. Additionally, our analysis focused on epithelial and T cell subsets, while other critical players in the tumor microenvironment—such as fibroblasts, myeloid cells, and endothelial cells—were not examined in detail. Finally, given the cross-sectional nature of our data, dynamic changes over time or in response to therapy could not be assessed. Future studies integrating temporal data, multi-omics modalities, and functional perturbation experiments will be essential to validate and expand upon our findings.

5 Conclusion

In conclusion, this study provides a detailed single-cell and spatial atlas of epithelial and T cell interactions in CRC, uncovering key communication pathways and cellular niches that may shape tumor immunity and progression. These insights lay the groundwork for further mechanistic studies and the development of targeted immunotherapeutic strategies.

Acknowledgements
Not applicable.

Author contributions
YZZ and YRN wrote the main manuscript text and LXY prepared figures. All authors reviewed the manuscript.

Funding
DeclarationNo funding was received for this study.

Data availability
All data generated in this study are included in this published article. Any additional information required to reanalyze the data reported in this paper is available from the lead contact upon request.

Declarations

Ethics approval and consent to participate
The data utilized in this study were sourced from publicly accessible databases and were managed under approved ethical exemptions.

Consent for publication
The authors agreed to publication in the journal.

Competing interests
The authors declare no competing interests.

Received: 19 July 2025 / Accepted: 11 November 2025
Published online: 28 November 2025

References

1. Dekker E, Tanis PJ, Vleugels JLA, Kasi PM, Wallace MB. Colorectal cancer. Lancet (London England). 2019;394(10207):1467–80.
2. Biller LH, Schrag D. Diagnosis and treatment of metastatic colorectal cancer: a review. JAMA. 2021;325(7):669–85.
3. Nguyen LH, Goel A, Chung DC. Pathways of colorectal carcinogenesis. Gastroenterology. 2020;158(2):291–302.
4. Nicolini A, Ferrari P. Involvement of tumor immune microenvironment metabolic reprogramming in colorectal cancer progression, immune escape, and response to immunotherapy. Front Immunol. 2024;15:1353787.
5. Bian S, Hou Y, Zhou X, Li X, Yong J, Wang Y, et al. Single-cell multiomics sequencing and analyses of human colorectal cancer. Sci (New York NY). 2018;362(6418):1060–3.
6. Joanito I, Wirapati P, Zhao N, Nawaz Z, Yeo G, Lee F, et al. Single-cell and bulk transcriptome sequencing identifies two epithelial tumor cell States and refines the consensus molecular classification of colorectal cancer. Nat Genet. 2022;54(7):963–75.
7. Lizarralde-Guerrero M, Zucaro L, Kroemer G, Pol JG. Single-cell analysis of T lymphocytes infiltrating colorectal carcinoma: the dilemma of specificity. Oncoimmunology. 2024;13(1):2300520.
8. Xu M, Zhang G, Cui T, Liu J, Wang Q, Shang D, et al. Cross-modal integration of bulk RNA-seq and single-cell RNA sequencing data to reveal T-cell exhaustion in colorectal cancer. J Cell Mol Med. 2024;28(18):e70101.
9. Du J, Yang YC, An ZJ, Zhang MH, Fu XH, Huang ZF, et al. Advances in Spatial transcriptomics and related data analysis strategies. J Translational Med. 2023;21(1):330.
10. Lee HO, Hong Y, Etlioglu HE, Cho YB, Pomella V, Van den Bosch B, et al. Lineage-dependent gene expression programs influence the immune landscape of colorectal cancer. Nat Genet. 2020;52(6):594–603.
11. Satija R, Farrell JA, Gennert D, Schier AF, Regev A. Spatial reconstruction of single-cell gene expression data. Nat Biotechnol. 2015;33(5):495–502.
12. Korsunsky I, Millard N, Fan J, Slowikowski K, Zhang F, Wei K, et al. Fast, sensitive and accurate integration of single-cell data with harmony. Nat Methods. 2019;16(12):1289–96.
13. Kang M, Armenteros JJA, Gulati GS, Gleyzer R, Avagyan S, Brown EL, et al. Mapping single-cell developmental potential in health and disease with interpretable deep learning. bioRxiv. 2024. https://doi.org/10.1101/2024.03.19.585637.
14. Street K, Risso D, Fletcher RB, Das D, Ngai J, Yosef N, et al. Slingshot: cell lineage and pseudotime inference for single-cell transcriptomics. BMC Genomics. 2018;19(1):477.
15. Chen K, Wang Y, Hou Y, Wang Q, Long D, Liu X, et al. Single cell RNA-seq reveals the CCL5/SDC1 receptor-ligand interaction between T cells and tumor cells in pancreatic cancer. Cancer Lett. 2022;545:215834.
16. Wu T, Hu E, Xu S, Chen M, Guo P, Dai Z, et al. ClusterProfiler 4.0: A universal enrichment tool for interpreting omics data. Innov (Cambridge (Mass). 2021;2(3):100141.
17. Li X, Zhou Y, Jiang Q, Huang J, Liu Z, Li Y, et al. A novel scoring model based on RNA modification writers can predict the prognosis and guide immunotherapy in gastric cancer. Funct Integr Genom. 2023;23(2):162.
18. Jin S, Guerrero-Juarez CF, Zhang L, Chang I, Ramos R, Kuan CH, et al. Inference and analysis of cell-cell communication using cellchat. Nat Commun. 2021;12(1):1088.
19. Cui K, Gao X, Wang B, Wu H, Arulsamy K, Dong Y, et al. Epsin nanotherapy regulates cholesterol transport to fortify atheroma regression. Circul Res. 2023;132(1):e22–42.
20. Wei R, He S, Bai S, Sei E, Hu M, Thompson A, et al. Spatial charting of single-cell transcriptomes in tissues. Nat Biotechnol. 2022;40(8):1190–9.
21. Heiser CN, Simmons AJ, Revetta F, McKinley ET, Ramirez-Solano MA, Wang J, et al. Molecular cartography uncovers evolutionary and microenvironmental dynamics in sporadic colorectal tumors. Cell. 2023;186(25):5620–e56375616.
22. Cañellas-Socias A, Cortina C, Hernando-Momblona X, Palomo-Ponce S, Mulholland EJ, Turon G, et al. Metastatic recurrence in colorectal cancer arises from residual EMP1(+) cells. Nature. 2022;611(7936):603–13.
23. Roelands J, van der Ploeg M, Ijsselsteijn ME, Dang H, Boonstra JJ, Hardwick JCH, et al. Transcriptomic and immunophenotypic profiling reveals molecular and immunological hallmarks of colorectal cancer tumourigenesis. Gut. 2023;72(7):1326–39.
24. Mei Y, Xiao W, Hu H, Lu G, Chen L, Sun Z, et al. Single-cell analyses reveal suppressive tumor microenvironment of human colorectal cancer. Clin Translational Med. 2021;11(6):e422.
25. Hartmann FJ, Mrdjen D, McCaffrey E, Glass DR, Greenwald NF, Bharadwaj A, et al. Single-cell metabolic profiling of human cytotoxic T cells. Nat Biotechnol. 2021;39(2):186–97.
26. Ding JT, Yang KP, Zhou HN, Huang YF, Li H, Zong Z. Landscapes and mechanisms of CD8(+) T cell exhaustion in gastrointestinal cancer. Front Immunol. 2023;14:1149622.
27. Beauchemin N, Arabzadeh A. Carcinoembryonic antigen-related cell adhesion molecules (CEACAMs) in cancer progression and metastasis. Cancer Metastasis Rev. 2013;32(3–4):643–71.
28. Jiang Y, Long G, Huang X, Wang W, Cheng B, Pan W. Single-cell transcriptomic analysis reveals dynamic changes in the liver microenvironment during colorectal cancer metastatic progression. J Translational Med. 2025;23(1):336.
29. Zhou L, Wen R, Bai C, Li Z, Zheng K, Yu Y, et al. Spatial transcriptomic revealed intratumor heterogeneity and cancer stem cell enrichment in colorectal cancer metastasis. Cancer Lett. 2024;602:217181.

30. Pinkert J, Boehm HH, Trautwein M, Doecke WD, Wessel F, Ge Y, et al. T cell-mediated elimination of cancer cells by blocking CEACAM6-CEACAM1 interaction. Oncoimmunology. 2022;11(1):2008110.

Publisher's note